Inorganic Chemistry

Article

pubs.acs.org/IC

An Unnoticed Inorganic Solid Electrolyte: Dilithium Sodium Phosphate with the Nalipoite Structure

María C. López,[†] Gregorio F. Ortiz,*[,†] Elena M. Arroyo-de Dompablo,[‡] and José L. Tirado[†]

[†]Inorganic Chemistry Laboratory, University of Córdoba, Campus of Rabanales, Marie Curie Building, Cordoba E-14071, Spain

[‡]MALTA-Consolider Team, Departamento de Química Inorgánica, Facultad de Ciencias Químicas, Universidad Complutense de Madrid, 28040 Madrid, Spain

Supporting Information

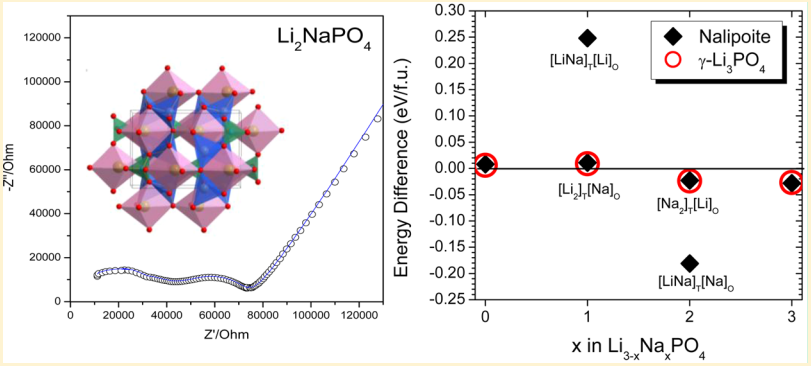

ABSTRACT: Solid electrolytes are crucial in the development of advanced lithium batteries and related technologies. Orthorhombic Li_2NaPO_4 (nalipoite) was synthesized, and its ionic conductivity compared very favorably with that of Li_3PO_4. The potential applicability of $Li_{3-x}Na_xPO_4$ as a lithium ion solid electrolyte was investigated for first time. First-principles DFT calculations were used to evaluate the possibilities of preparing other crystal structures.

INTRODUCTION

Lithium phosphates are promising candidates as lithium ionic conductor materials for high-energy batteries and other related technologies. Indeed, they are materials permeable to lithium ions and impermeable to electrons, which serve as good candidates for solid electrolytes. In addition, they are lightweight and have a wide potential range of stability versus lithium and lithium-containing electrodes. Nevertheless, lithium phosphate electrolytes have not been used in practical lithium ion batteries because their ionic conductivities are generally lower than those of superionic conductors (10^{-2} S cm^{-1})[1] and do not meet the required current densities. Chemical modifications of Li_3PO_4 might result in interesting ionic conductors. For instance, like lithium phosphate, Li_2NaPO_4 (nalipoite) can be used in thin films because of its chemical and physical stability. Moreover, the preparation of different Na-substituted Li_3PO_4 compounds could lead to novel sodium conductors, as Na_3PO_4 rapidly conducts sodium ions. To date, little has been reported about the synthesis and electronic properties of the $Li_{3-x}Na_xPO_4$ family of compounds, of which the x = 0, 1, 2, and 3 members are known to exist.[2]

It is known that there are three crystalline forms of Li_3PO_4, which are labeled as α, β, and γ.[3−6] They all consist of [PO_4] tetrahedra connected by corners and/or edges with [LiO_4] tetrahedra. Density functional theory (DFT) calculations have shown that the γ-Li_3PO_4-related form (space group $P2_1/n$) is about 60 meV per formula unit (f.u.) less stable than the β-Li_3PO_4 derivatives at 0 K (space groups $Pmnb$ and $Pmn2_1$).[7] The conductivities of the β and γ forms at 25 °C have been reported as 8.62×10^{-8} and 4.2×10^{-18} S cm^{-1}, respectively.[8,9] While there have been a large number of reports dealing with the study of Li_3PO_4 polymorphs, Li_2NaPO_4 has been proportionally considered in less detail. Dilithium sodium phosphate (Li_2NaPO_4, nalipoite) is new mineral species from Mont Saint-Hilaire, Quebec.[10] Its structure was resolved by T. S. Ercit in 1991.[11] To the best of our knowledge, no data reporting the ionic conductivity of this composition are found in the literature. For the sake of clarity, the unit cell structure is depicted in Figure 1. The structure has three oxygen-coordinated sites. P and Li are tetrahedrally coordinated, while Na is octahedrally coordinated. Each corner of each PO_4 tetrahedron is shared with two Li atoms. The PO_4 and LiO_4 tetrahedra form a corner-linked framework based on a stacking of two-dimensional nets. Na occupies the cages resulting from the three-dimensional network. On this assumption, we think it necessary to follow research lines on phosphate materials as major alternatives that may be suitable for better performance and compatibility of electrode−electrolyte interfaces in lithium batteries.

Received: December 12, 2013
Published: February 6, 2014

   dx.doi.org/10.1021/ic4030537 | Inorg. Chem. 2014, 53, 2310−2316

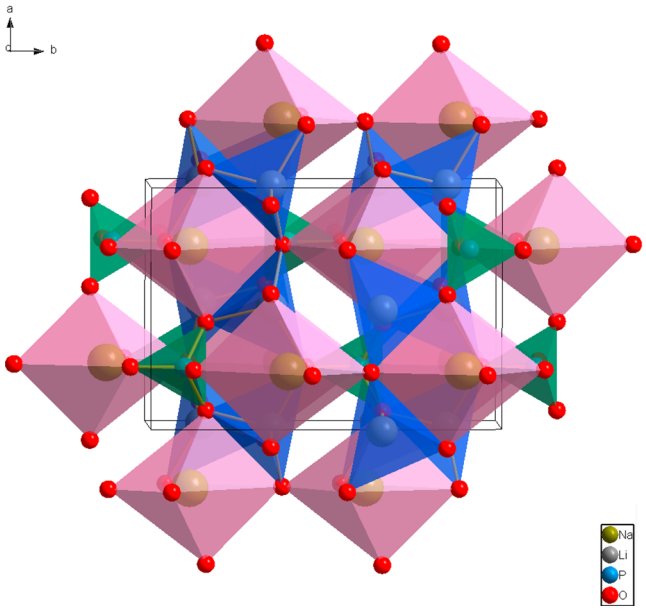

Figure 1. Description of the Li_2NaPO_4 unit cell in the *ab* plane, showing PO_4 tetrahedra (green), LiO_4 tetrahedra (blue), and NaO_6 distorted octahedra (pink).

The effect of mixing monovalent ions in crystalline ion conductors has been very fruitful in some situations. For example, the superionic transition temperature in AgI was decreased by partial replacement of silver by rubidium.[12] We expected to improve the ionic conductivity of Li_3PO_4 by Na substitution. With this aim, we attempted to prepare several members of the $Li_{3-x}Na_xPO_4$ family to explore their ionic conductivity. A novel wet-chemical method followed by optimal thermal treatment was designed to prepare nalipoite Li_2NaPO_4. The experimental impedance analyses allow practical ionic conductivities for pure nalipoite to be obtained, and they are 2 orders of magnitude higher than that of Li_3PO_4. We will show that the nalipoite phase displays better lithium ion mobility than any of the Li_3PO_4 forms.

The good ionic conductivity found in nalipoite Li_2NaPO_4 made it appealing to explore novel polymorphs of the compounds $Li_{3-x}Na_xPO_4$ ($0 < x < 3$). With this aim, first-principles DFT calculations were used to investigate the relative thermodynamic stabilities of $Li_{3-x}Na_xPO_4$ compounds within the crystal structures of nalipoite, γ-Li_3PO_4, and β-Li_3PO_4. The present work serves as one more brick for the scientific community to develop and discuss new perspectives in designing new chemistries.

METHODOLOGY

In order to obtain the $Li_{3-x}Na_xPO_4$ ($0 \le x \le 3$) series, $LiOH{\cdot}H_2O$ (Panreac, purity ≥98%), NaOH (Panreac, purity ≥98%), and H_3PO_4 (Panreac, purity ≥86%) were mixed in the appropriate proportions as starting materials. The advantage of using wet-chemical methods is that they can accommodate comparatively small amounts of a sample in diverse shapes or forms. The order of addition of the reagents to the aqueous solution was revealed to be important. For example, to obtain Li_2NaPO_4, a 0.1 M solution of NaOH in distilled water was mixed with 0.1 M H_3PO_4 and then 0.2 M LiOH was added dropwise. Next, the mixture was stirred vigorously and dried at 100 °C in air overnight. To further optimize the synthesis of nalipoite Li_2NaPO_4, several temperatures from 500 to 1000 °C were tested, having in mind that the β-Li_3PO_4 phase is obtained directly by precipitation of LiOH and H_3PO_4 at 500 °C. The samples were naturally cooled to room temperature in 4 h.

The phase formation was studied by powder X-ray diffraction (PXRD) on a Siemens D5000 diffractometer with Cu Kα radiation operating at 40 kV and 30 mA. The samples were scanned between 2θ = 10 and 110° in step scan mode in steps of 0.02°/10 s. Unit cell parameters were calculated using Fullprof software. FTIR data were obtained with a Bruker Tensor 27 FT-MIR spectrophotometer with CsI beam splitters and a DTGS detector. OPUS version 6.5 software was used to collect the transmission spectra.

Electrochemical impedance spectroscopy (EIS) measurements were performed with an Autolab PGSTAT12 system by applying an AC signal with an amplitude of 5 mV over the frequency range from 1 MHz to 100 mHz. The electrodes were prepared by pressing the active material into 10 mm diameter discs at 5 tons. The pellets were sintered at 300−1000 °C in an atmosphere of air for 30 h and then slowly cooled to room temperature. The annealed electrodes were assembled in Swagelok-type two-electrode cells. A silver conducting paste was used to ensure electrical connectivity to both stainless steel current collectors. The impedance spectra were transformed into Nyquist plots. The plots were used to fit the parameters of an equivalent circuit consisting of $(R_bQ_b)(R_{gb}Q_{gb})(Q_{el})$, where R is the resistance, Q is the constant phase element, and the subscripts el, b, and gb refer to the electrode, bulk, and grain boundary, as described elsewhere.[13,14] The ionic conductivity was calculated as $\sigma = L/RA$, where L and A are the thickness and area of the pellet, respectively. In addition, possible hygroscopicity issues were also minimized by predrying the prepared pellets before cell assembly in an inert atmosphere.

The total energies of $Li_{3-x}Na_xPO_4$ ($0 \le x \le 3$) polymorphs were calculated using the projector augmented wave (PAW)[15,16] formalism as implemented in the Vienna Ab Initio Simulation Package (VASP),[17] with the exchange and correlation energies approximated using the generalized gradient approximation (GGA). For the exchange and correlation functional, we choose a form suggested by Perdew, Burke, and Ernzerhof (PBE).[18] The wave functions were expanded with a plane-wave basis set with a cutoff kinetic energy of 600 eV. The integration in the Brillouin zone was done using the tetrahedron method as corrected by Blöchl on a set of k points ($6 \times 6 \times 6$ for the β form and $6 \times 4 \times 6$ for the γ and nalipoite polymorphs) determined by the Monkhorst−Pack scheme. With these parameters, a total-energy convergence close to 4 meV/f.u. was achieved. The initial cell

Table 1. Refined Unit Cell Parameters and Cell Volumes of Lithium Phosphate and Nalipoite Samples Utilized for Conductivity Measurements, with Computational Data Given in Parentheses

	space group	a (Å)	b (Å)	c (Å)	V (Å^3)
β-Li_3PO_4 (RT)	$Pmn2_1$	6.1325(6)	5.2446(4)	4.8791(4)	156.92(3)
		(6.159)	(5.282)	(4.981)	(159.16)
β-Li_3PO_4 (300 °C)	$Pmn2_1$	6.1251(6)	5.2400(3)	4.8582(4)	155.92(2)
γ-Li_3PO_4 (500 °C)	$Pmnb$	6.1135(3)	10.4726(2)	4.8865(4)	312.85(4)
		(6.151)	(10.563)	(4.971)	(323.01)
Li_2NaPO_4 (700 °C)	$Pmnb$	6.8751(1)	9.9888(3)	4.9315(6)	338.66(8)
		(6.855)	(10.146)	(4.975)	(346.02)

dx.doi.org/10.1021/ic4030537 | Inorg. Chem. 2014, 53, 2310−2316

parameters and atomic positions of β-Li_3PO_4 and γ-Li_3PO_4 were taken from refs 4 and 8, respectively. The initial structure of the nalipoite corresponded to the model described by Ercit.[11] The structures were fully relaxed (cell parameters, cell volumes, and atomic positions), and the final energies of the optimized geometries were recalculated in order to correct for the changes in the basis set of the wave functions during relaxation. For Li_3PO_4 and Li_2NaPO_4 polymorphs, relaxed structure calculations were performed at various constant volumes, and the energy−volume data were fitted to the Murnaghan equation of state.[19]

RESULTS AND DISCUSSION

(a). Crystal Stability and Synthesis of $Li_{3-x}Na_xPO_4$ Compounds. As a starting point, we investigated possible crystal structures for the compounds $Li_{3-x}Na_xPO_4$ (x = 0, 1, 2, 3) by DFT methods. The candidate crystal structures were those adopted by nalipoite Li_2NaPO_4, γ-Li_3PO_4, and β-Li_3PO_4. In nalipoite Li_2NaPO_4, the Li and Na ions occupy tetrahedral and octahedral sites, respectively (see Figure 1). Thus, for the A_2BPO_4 compositions we considered two possible distributions of ions: $[A,B]_T[A]_O$ and $[A,A]_T[B]_O$. Calculated lattice parameters for the existing compounds β-Li_3PO_4, γ-Li_3PO_4, and nalipoite Li_2NaPO_4 are compared to the experimental

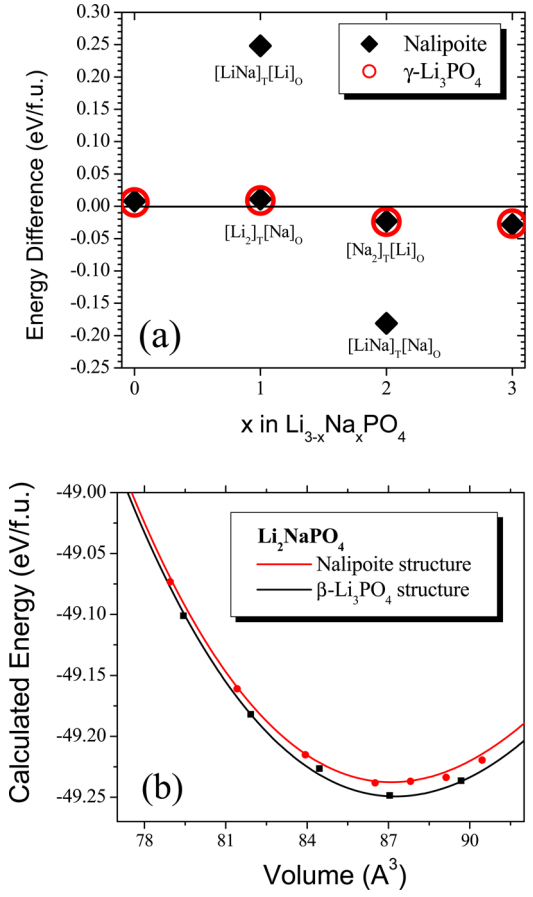

Figure 2. (a) Relative stabilities of $Li_{3-x}Na_xPO_4$ (x = 0, 1, 2, 3) having the crystal structures of nalipoite Li_2NaPO_4, γ-Li_3PO_4, and β-Li_3PO_4. The calculated total energy for β-Li_3PO_4 is set as the zero of energy. (b) Plots of total energy vs volume for the Li_2NaPO_4 composition with the β-Li_3PO_4 and nalipoite structures. Symbols correspond to the DFT-calculated data, and lines show the fits to the Murnagham equation of state. The values of the fit parameters are given in Table S1 in the Supporting Information.

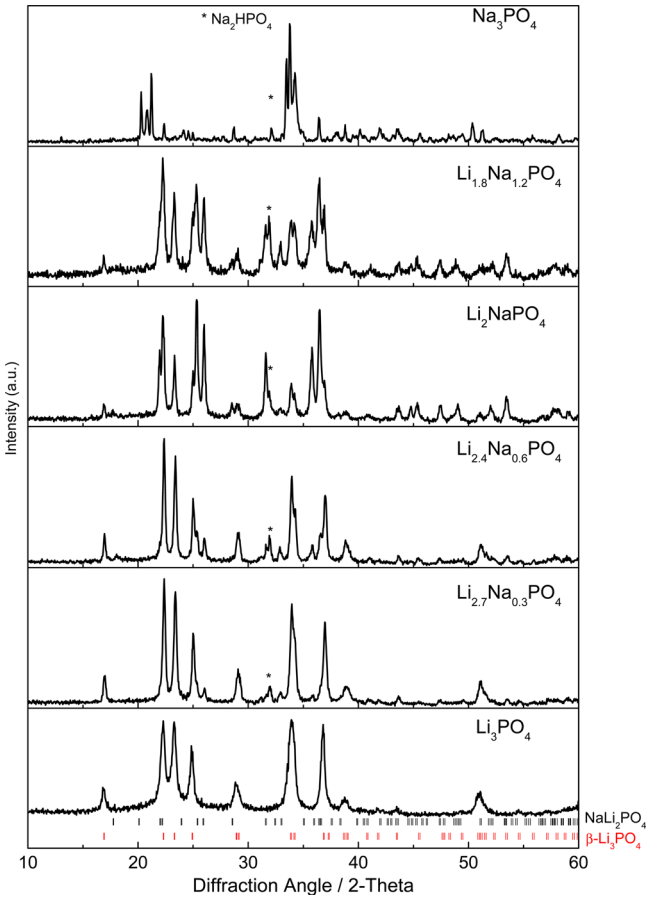

Figure 3. PXRD patterns of $Li_{3-x}Na_xPO_4$ ($0 \leq x \leq 3$) samples prepared at room temperature.

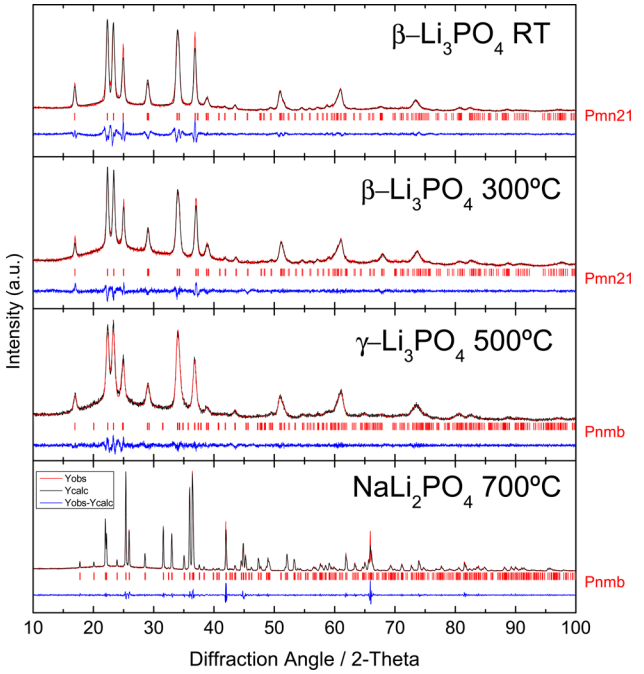

Figure 4. Comparison of the PXRD patterns of Li_3PO_4 forms: the low-temperature form (β-phase) at RT and 300 °C, the medium-temperature form (γ-phase), and the high-temperature form (Li_2NaPO_4). The fits were performed with Fullprof software using published crystallographic data.[4,8,21]

dx.doi.org/10.1021/ic4030537 | Inorg. Chem. 2014, 53, 2310−2316

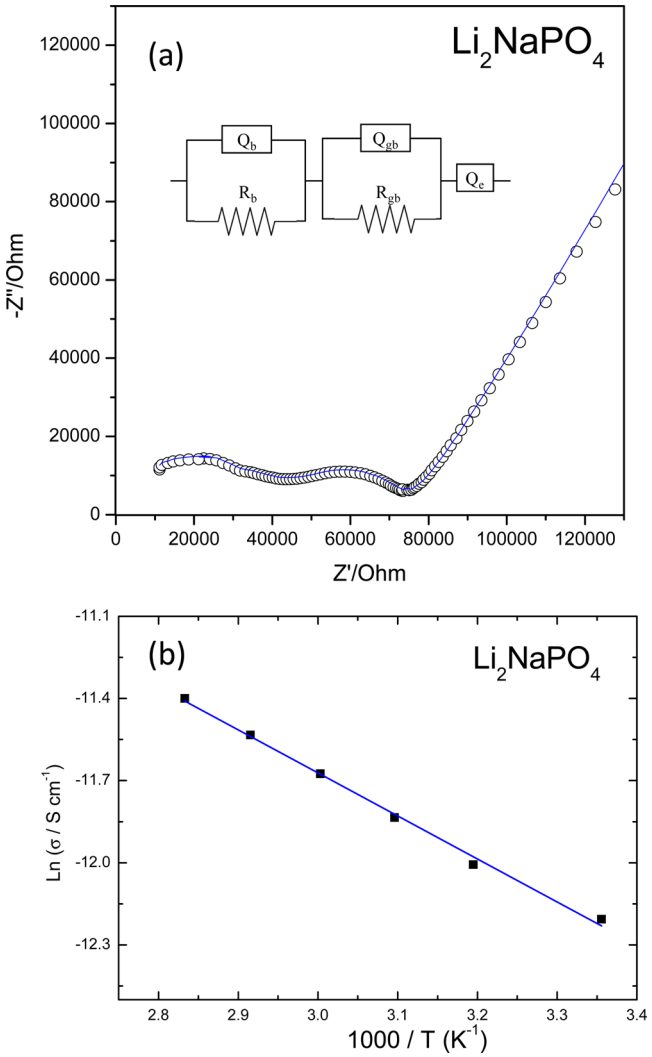

Figure 5. (a) EIS data recorded for Li_2NaPO_4. The experimental values (○) were fitted to an equivalent circuit consisting of $(R_bQ_b)(R_{gb}Q_{gb})(Q_{el})$. (b) Arrhenius plot for the bulk total electrical conductivity of Li_2NaPO_4.

values in Table 1. The errors are on the order of 3%, which affirms the validity of the calculation method.

Figure 2a shows the relative stabilities of $Li_{3-x}Na_xPO_4$ (x = 0, 1, 2, 3) having the three investigated structures, with the total energy of the β-Li_3PO_4 structure set as the zero of energy. The computational results indicate that for Li_3PO_4 the β form is the stable polymorph, in good agreement with previous experimental and computational reports.[5,7] The β-Li_3PO_4 form is also predicted as the most stable polymorph for the Li_2NaPO_4 composition, though with a small energy difference (10 meV/f.u.) relative to the nalipoite $[Li_2]_T[Na]_OPO_4$ and γ-Li_3PO_4 polymorphs. The virtual nalipoite $[Li,Na]_T[Li]_OPO_4$ structure is by far less stable than the β polymorph (250 meV/f.u.). At higher Na contents, the β-Li_3PO_4 structural type becomes destabilized in favor of the nalipoite and γ-Li_3PO_4 structures. This is not surprising since in these structures distorted octahedral sites are available to accommodate the larger Na cations. It is noteworthy that for $LiNa_2PO_4$ the cationic distribution $[Li,Na]_T[Na]_O$ is particularly stable relative to the β-Li_3PO_4 form.

Figure 2b shows the fits of the energy−volume data at 0 K to the Murnaghan equation of state for the Li_2NaPO_4 composition having the nalipoite $[Li_2]_T[Na]_OPO_4$ and β-Li_3PO_4 structures. In view of Figure 2b, β-Li_3PO_4 is predicted as the stable form at any pressure at 0 K. However, the energy difference between nalipoite and β-Li_3PO_4 structures is small, and entropic contributions above 0 K might reverse the relative free energies. This is consistent with the fact that the nalipoite form is obtained experimentally while the β-Li_3PO_4 structure might not be observed at any temperature.

We attempted to prepare several members of the $Li_{3-x}Na_xPO_4$ family. The PXRD patterns of the samples obtained at room temperature are shown in Figure 3. The β-Li_3PO_4 (x = 0) phase was successfully obtained by precipitation of LiOH and H_3PO_4 at room temperature (PDF file no. 45-1348, orthorhombic). The Li-free sample (x = 3) is most likely a Na_3PO_4 phase that presented hydrated products in the final composition, which is indicative of the difficulty in preparing anhydrous Na_3PO_4 at room temperature.[20] Annealing this sample at 700 °C resulted in well-crystallized cubic sodium phosphate (γ-Na_3PO_4, PDF file no. 31-1318) accompanied by traces of the tetragonal phase (α-Na_3PO_4, PDF file no. 31-1323) (Figure S1 in the Supporting Information). For the intermediate compositions $Li_{3-x}Na_xPO_4$ with x = 0.3, 0.6, 1, and 1.2, the obtained powders exhibited XRD patterns corresponding to mixtures of β-Li_3PO_4 and nalipoite Li_2NaPO_4, with different ratios for the different x values. Thus, a pure Li_2NaPO_4 phase could not be obtained at room temperature.

From a thermodynamic point of view, it is known that the phase transformation from β- to γ-Li_3PO_4 occurs upon simple thermal treatment in air at 500−600 °C.[4,5,7,9] Also, it is known that the γ-Li_3PO_4 phase is defined by the same space group as Li_2NaPO_4 (*Pmnb*) and that both have orthorhombic cell parameters (Z = 4). With these aspects in mind, the effects of temperature on the crystal structure of the as-prepared Li_2NaPO_4 were studied in depth. Upon modulation of the temperature, it was possible to obtain pure and highly crystalline Li_2NaPO_4 (PDF file no. 45-1348) solely at 700 °C (see Figure S2 in the Supporting Information). At lower (500−600 °C) and higher (800−1000 °C) temperatures, nalipoite coexists with β- and γ-Li_3PO_4-like impurities. This phase stability competition is consistent with the result that the computed total energies were very close for the three structural types.

The above results show that both Li_2NaPO_4 and Na_3PO_4 can be purified by annealing at 700 °C in air. Further work to elucidate the synthesis conditions for the intermediate compositions $Li_{3-x}Na_xPO_4$ ($1 < x < 3$) is in progress. According to the DFT results, $Li_{3-x}Na_xPO_4$ compounds with high Na content could be stable in structures possessing octahedral sites. In particular, the composition $LiNa_2PO_4$ (i.e., x = 2) is very appealing from the point of view of lattice stability. Essays to prepare this composition were unsuccessful, and to the best of our knowledge, no mineral with this stoichiometry has been found in nature, in contrast to nalipoite. Moreover, the ionic conduction properties of Li_2NaPO_4 were found to be particularly attractive, as discussed below.

Figure 4 shows the PXRD refinements of the samples utilized for the conductivity measurements: nalipoite Li_2NaPO_4, γ-Li_3PO_4, and β-Li_3PO_4 at 300 °C and β-Li_3PO_4 at RT. The profile-only fitting was performed with Fullprof software. Table 1 summarizes the refined lattice parameters. Good agreement with those reported in the literature is observed.[4,8,21] The expansion in unit cell volume necessary to accommodate the larger Na^+ ions also increases the volume of interstitial space in

dx.doi.org/10.1021/ic4030537 | Inorg. Chem. 2014, 53, 2310−2316

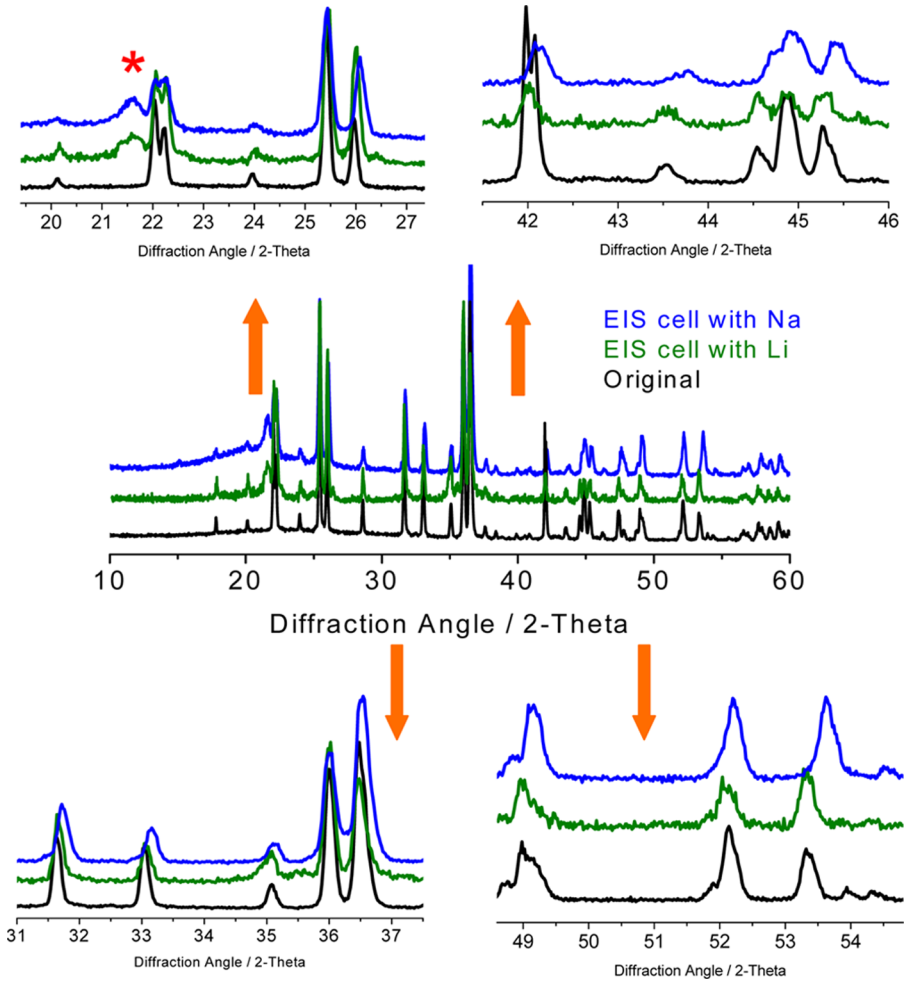

Figure 6. PXRD patterns of Li_2NaPO_4 recorded after EIS measurements between sodium (blue lines) and between lithium (green lines). The patterns are compared with that of the original Li_2NaPO_4 sample (black lines). Selected areas have been selected for better comparison of the X-ray patterns. The asterisk symbol is assigned to the plastic covering the sample holder.

nalipoite. This difference may provide easier pathways for lithium cation diffusivity and enhanced ionic conductivity in nalipoite.

(b). Ionic Conductivity. In order to evaluate the effects on the ionic conductive properties of the alkali metal mixture found in Li_2NaPO_4, electrochemical impedance spectra were recorded. The impedance plot and the fitted curve (solid line) obtained for nalipoite at RT are shown in Figure 5a, and the corresponding equivalent circuit is depicted in the inset. The Nyquist plot shows two semicircles at high and intermediate frequencies representing the bulk and grain-boundary resistances, respectively. The linear portion of the plot at low frequencies represents the blocking electrode. This long tail suggests that the material is an ionic conductor.[22,23] The bulk and grain-boundary resistances could be well-resolved from the fitting. Hence, the bulk (σ_b) and grain boundary (σ_{gb}) conductivities of Li_2NaPO_4 were found to be 6.5×10^{-6} and 1.9×10^{-6} S cm^{-1}, respectively. These values are higher than the value found for our synthesized γ-Li_3PO_4 (4×10^{-7} S cm^{-1}), β-Li_3PO_4 at 300 °C (1.2×10^{-7} S cm^{-1}), and β-Li_3PO_4 at RT (8×10^{-8} S cm^{-1}) (see Figure S3 in the Supporting Information). An outstanding result is that the total conductivity value reported for nalipoite is about 2 orders of magnitude higher than those of the other lithium phosphates reported in this work and in other works found in the literature, including the value of 8.62×10^{-8} S cm^{-1} for β-Li_3PO_4 prepared by electrodeposition on Pt and annealed at 300 °C, the value of 7×10^{-8} S cm^{-1} for Li_3PO_4 deposited by sputtering in Ar + O_2 ambiance, and the value of 2.4×10^{-8} S cm^{-1} for a Li_3PO_4-based composite electrolyte (Li_3PO_4:SiO_2:DBP:PVDF = 30:5:30:35 w/w/w/w).[9,24,25] The conductivity results presented here are still several orders of magnitude lower than those of liquid electrolytes. Compared with other systems of ionic conductors that have attracted great recent research interest, such as β-Li_3PS_4 (1.6×10^{-4} S cm^{-1} at RT),[26] $Li_{10}GeP_2S_{12}$ (1.2×10^{-3} S cm^{-1} at RT),[27] and $Li_{10}SnP_2S_{12}$ (4×10^{-3} S cm^{-1} at 27 °C),[28] the current Li_2NaPO_4 material is less interesting merely considering the ionic conductivity (6.5×10^{-6} S cm^{-1} at RT). This value is even lower than that of LiPON, which is produced by nitridation of Li_3PO_4 and is generally employed in solid-state thin-film lithium ion microbatteries.[29] An ideal solid-state lithium conductor not only should have high ionic conductivity at the operating temperature but also should be easy and cheap to prepare. LIPON is produced with expensive tools, and production on a large scale would be tedious in industry, assuming stratospheric costs. Another drawback is that Ge atoms in the above-mentioned lithium thiophosphate structure compromise the chemical compatibility of the lithium thiophosphate with lithium metal.[30] An ideal solid-state lithium

dx.doi.org/10.1021/ic4030537 | Inorg. Chem. 2014, 53, 2310−2316

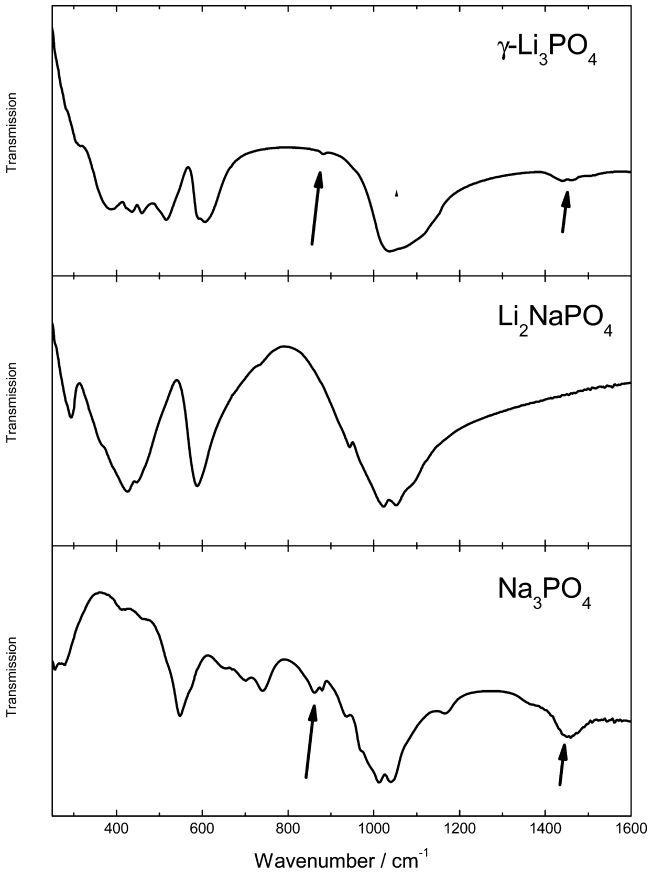

Figure 7. IR spectra of (a) γ-Li_3PO_4, (b) nalipoite Li_2NaPO_4, and (c) napoite Na_3PO_4.

ion conductor should show evidence of the following properties: (i) stability against chemical reactions with the anode and cathode; (ii) thermal stability in air up to the annealing temperature; (iii) low cost; (iv) absence of water in the material; and (v) environmental benignancy.[31] Most of the materials mentioned above do not meet all of these requirements. Nanoporous lithium thiophosphate materials have emerged as alternative solid electrolytes with ionic conductivities several orders of magnitude above phosphates, but mostly by surface conduction of β-Li_3PS_4 due to the high surface-to-bulk ratio.[26]

An interesting observation is that the grain-boundary contribution to the total nalipoite resistance is less than 50% at room temperature. When impedance measurements are performed at higher temperatures (>50 °C), it is difficult to separate the bulk and grain-boundary contributions for the determination of the electrical conductivity over the temperature range investigated (25−70 °C). Similar behavior was found by other authors in the study of ionic-conductive garnets.[22] The temperature dependence of the conductivity for a Li_2NaPO_4 sample showed Arrhenius-type behavior (Figure 5b). A significant improvement from the value observed at RT (6.5×10^{-6} S cm^{-1}) was observed at 70 °C, where a total conductivity of ca. 1.5×10^{-5} S cm^{-1} was reached. However, the lithium ion conduction activation energy calculated from the Arrhenius plot was about ~0.23 eV, which is relatively low compared with other data reported in the literature. For instance, in their QENS study Wilmer and Meyer reported activation energies of 0.18 and 0.75 eV for PO_4 rotation and Na^+ jumps, respectively.[32] Furthermore, the activation energies for Li^+ ions in LISICONs (0.5 eV) are not much lower either.[31] For solid electrolytes based on lithium titanium phosphates, activation energies of about 0.35 and 0.20 eV at low and high (>473 K) temperatures, respectively, were reported.[33]

The low activation energies reported here may suggest that only a fraction of the ions are mobile in Li_2NaPO_4. A first assumption could be that oxygen, phosphorus, and sodium species are rigidly bound in the framework of the structure and have negligible mobility at operating temperatures, and hence, the ionic motion would be due to the transport of Li^+ ions. Unlike the case with aliovalent doping into Na_3PO_4,[34] there is no obvious increase in the number of lattice sites (vacancies) available for Na^+ or Li^+ diffusion, since Li_2NaPO_4 is structurally similar to the end members Li_3PO_4 and Na_3PO_4. To check this assumption, the structure of the solid was reexamined after EIS measurement versus Li and Na electrodes. Figure 6 shows an X-ray diffraction pattern exhibiting a shift of the peaks for the case of the Na cells compared with the original sample. We found that no significant changes in the lattice parameters resulted from Li cells, thus confirming the lack of ionic motion for Na. In contrast, the Na cell produced shifts in the spacing that suggest displacement of Li from the structure and hence its replacement with Na^+ occupying new sites, which is a sign of Li cation mobility in the structure. A Rietveld analysis of the electrolyte used in sodium cells revealed that the occupancy of Li 8d sites had become ca. 75% Li and 25% Na. However the unit cell parameters showed a decrease in cell volume (335.98 Å^3) after use in the Na cell. This change is difficult to explain by simply taking into account the ionic radii of Li^+ and Na^+. A structural modification could account for this discrepancy. Further work on this question is now in progress, which is out of the scope of this paper.

An alternative explanation of the low activation energies could be that protons could be incorporated into M_3PO_4 (M = K, Li, Na),[35] contributing significantly to the total conductivity. In order to check this possibility, FTIR spectra of various M_3PO_4 polymorphs such as γ-Li_3PO_4, nalipoite Li_2NaPO_4, and napoite Na_3PO_4 were recorded (Figure 7). Three different zones should be indicative of hydrogen bonding and hence were carefully analyzed: (i) the appearance of ν(P−O−H) absorption bands for in-plane deformation at about 865−880 cm^{-1} and P−O−H stretching modes at 1443−1463 cm^{-1}; (ii) a shift in the $\nu_3(PO_4^{3-})$ stretching mode to lower wavenumbers; and (iii) broadening of the $\nu_4(PO_4^{3-})$ absorption bands at 560−618 cm^{-1} or broadening of the $\nu_2(PO_4^{3-})$ absorption bands at about 417 cm^{-1}.[36,37] Hydrogen bonding may exist in the crystal structures of Na_3PO_4 and probably in γ-Li_3PO_4, but for nalipoite Li_2NaPO_4 there is no clear evidence of hydrogen bonding. In this respect, the out-of-plane OH bending vibration of P−O−H usually appearing at 1230−1260 cm^{-1}, which is typical for $NaH_5(PO_4)_2$ related compounds,[38] would also be useful for understanding that protons are not visible in our nalipoite Li_2NaPO_4 phase.

It should further be noted that the incorporation of various ions (Na^+, Ca^{2+}, Fe^{3+}) into the crystal lattice of phosphate compounds may lead to significant changes in their ionic[39,40] or electrical conductivities[41] and some cases shift the potential reaction of the Ti^{4+}/Ti^{3+} redox couple in Li cells.[42] On this assumption, we think it necessary to follow the research lines close to phosphate materials, as they are one of the major alternatives suitable for better performance and compatibility of electrode−electrolyte interfaces.

dx.doi.org/10.1021/ic4030537 | Inorg. Chem. 2014, 53, 2310−2316

CONCLUSIONS

A simple and cheap way to prepare orthorhombic Li_2NaPO_4 powder involving a wet-chemical method followed by optimal thermal treatment at 700 °C was successfully developed. It is the first time that the ionic conductivity of Li_2NaPO_4 is reported, and values of 6.5×10^{-6} and 1.5×10^{-5} S cm^{-1} at 25 and 70 °C, respectively, were obtained. The conductivity value is higher than those of β- and γ-Li_3PO_4 phases by about 2 orders of magnitude, making Li_2NaPO_4 a very appealing candidate for future solid electrolytes in batteries. These results open new perspectives by finding alternative diffusion paths that allow enhanced lithium/sodium ionic conductors in the $Li_{3-x}Na_xPO_4$ family. DFT calculations were used to evaluate the thermodynamic stabilities of several polymorphs for this family. We found that for small x values (ca. $x < 1.5$), Na ions could be accommodated in the β-Li_3PO_4 network. Compounds with greater Na contents could be stable within crystal structures possessing octahedral sites.

ASSOCIATED CONTENT

Supporting Information

Calculated equation of state parameters for Li_2NaPO_4 polymorphs, PXRD patterns for $Li_{3-x}Na_xPO_4$, and impedance spectra of Li_3PO_4. This material is available free of charge via the Internet at http://pubs.acs.org.

AUTHOR INFORMATION

Corresponding Author

*E-mail: q72maorg@uco.es. Tel.: +34 957 21 86 37.

Notes

The authors declare no competing financial interest.

ACKNOWLEDGMENTS

We thank MEC-MAT 2011-22753, MEC-CSD2007-00045, and "Junta de Andalucía" (FQM-288 and FQM-7206) for financial support. G.F.O. is indebted to the "Ramón y Cajal" Program.

REFERENCES

(1) Dudney, N. J. In *Lithium Batteries: Science and Technology*; Nazri, G.-A., Pistoia, G., Eds.; Kluwer: Dordrecht, The Netherlands, 2004; pp 623−642.
(2) Zimina, G. V.; Smirnova, I. N.; Fomichev, V. V.; Zaitseva, M. G.; Kupenko, V. I. *Zh. Neorg. Khim.* **2005**, *50*, 744−749.
(3) Zemann, J. *Acta Crystallogr.* **1960**, *13*, 863−867.
(4) Keffer, C.; Mighell, A.; Mauer, F.; Swanson, H.; Block, S. *Inorg. Chem.* **1967**, *6*, 119−125.
(5) West, A. R.; Glasser, F. P. *J. Solid State Chem.* **1972**, *4*, 20−28.
(6) Baur, W. H. *Inorg. Nucl. Chem. Lett.* **1980**, *16*, 525−527.
(7) Arroyo-de Dompablo, M. E.; Dominko, R.; Gallardo-Amores, J. M.; Dupont, L.; Mali, G.; Ehrenberg, H.; Jamnik, J.; Moran, E. *Chem. Mater.* **2008**, *20*, 5574−5584.
(8) Wang, B.; Chakoumakos, B. C.; Sales, B. C.; Kwak, B. S.; Bates, J. B. *J. Solid State Chem.* **1995**, *115*, 313−323.
(9) Liu, H. C.; Yen, S. K. *J. Power Sources* **2006**, *159*, 245−248.
(10) Chao, G. Y.; Ercit, T. S. *Can. Mineral.* **1991**, *29*, 565−568.
(11) Ercit, T. S. *Can. Mineral.* **1991**, *29*, 569−573.
(12) Geller, S. *Acc. Chem. Res.* **1978**, *11*, 87−94.
(13) Xie, H.; Goodenough, J. B.; Li, Y. *J. Power Sources* **2011**, *196*, 7760−7762.
(14) Matsui, N. *Solid State Ionics* **1992**, *57*, 121−124.
(15) Blochl, P. E. *Phys. Rev. B.* **1994**, *50*, 17953−17979.
(16) Kresse, G.; Joubert, J. *Phys. Rev. B* **1999**, *59*, 1758−1775.
(17) Kresse, G.; Furthmüller, J. *Comput. Mater. Sci.* **1996**, *6*, 15−50.
(18) Perdew, J. P.; Burke, K.; Ernzerhof, M. *Phys. Rev. Lett.* **1996**, *77*, 3865−3868.
(19) Murnaghan, F. D. *Proc. Natl. Acad. Sci. U.S.A.* **1944**, *30*, 244−247.
(20) Ghule, A.; Baskaran, N.; Murugan, R.; Chang, H. *Solid State Ionics* **2003**, *161*, 291−299.
(21) Reculeau, E.; Elfakir, A.; Quarton, M. *J. Solid State Chem.* **1989**, *79*, 205−211.
(22) Murugan, R.; Thangadurai, V.; Weppner, W. *Angew. Chem., Int. Ed.* **2007**, *46*, 7778−7781.
(23) Kanno, R.; Hata, T.; Kawamoto, Y.; Irie, M. *Solid State Ionics* **2000**, *130*, 97−104.
(24) Yu, X.; Bates, J. B.; Jellison, G. E., Jr.; Hart, F. X. *J. Electrochem. Soc.* **1997**, *144*, 524−532.
(25) Zhang, S. Q.; Xie, S.; Chen, C. H. *Mater. Sci. Eng., B* **2005**, *121*, 160−165.
(26) Liu, Z.; Fu, W.; Payzant, E. A.; Yu, X.; Wu, Z.; Dudney, N. J.; Kiggans, J.; Hong, K.; Rondinone, A. J.; Liang, C. *J. Am. Chem. Soc.* **2013**, *135*, 975−978.
(27) Kamaya, N.; Homma, K.; Yamakawa, Y.; Hirayama, M.; Kanno, R.; Yonemura, M.; Kamiyama, T.; Kato, Y.; Hama, S.; Kawamoto, K.; Mitsui, A. *Nat. Mater.* **2011**, *10*, 682−686.
(28) Bron, P.; Johansson, S.; Zick, K.; auf der Gunne, J. S.; Dehnen, S.; Roling, B. *J. Am. Chem. Soc.* **2013**, *135*, 15694−15697.
(29) Mascaraque, N.; Fierro, J. L. G.; Durán, A.; Muñoz, F. *Solid State Ionics* **2013**, *233*, 73−79.
(30) Mo, Y.; Ong, S. P.; Ceder, G. *Chem. Mater.* **2012**, *24*, 15−17.
(31) Thangadurai, V.; Weppner, W. *Ionics* **2002**, *8*, 281−292.
(32) Wilmer, D.; Meyer, H. W. *Z. Phys. Chem.* **2009**, *223*, 1341−1357.
(33) Aono, H.; Sugimoto, E.; Sadaoka, Y.; Imanaka, N.; Adachi, G. *J. Electrochem. Soc.* **1990**, *137*, 1023−1027.
(34) Irvine, I. T. S.; West, A. R. *Solid State Ionics* **1988**, *28*, 214−219.
(35) Mellander, B. E.; Zhu, B. *Solid State Ionics* **1993**, *61*, 105−110.
(36) Chapman, A. C.; Thirlwell, L. E. *Spectrochim. Acta* **1964**, *20*, 937−947.
(37) Zhu, B.; Mellander, B. E.; Chen, J. *Mater. Res. Bull.* **1993**, *28*, 321−328.
(38) Baran, J.; Lis, T.; Drozd, M.; Ratajczak, H. *J. Mol. Struct.* **2000**, *516*, 185−202.
(39) Ortiz, G. F.; López, M. C.; Lavela, P.; Vidal-Abarca, C.; Tirado, J. L. *Solid State Ionics* **2013**, DOI: 10.1016/j.ssi.2013.09.012.
(40) Irvine, J. T. S.; West, A. R. *Solid State Ionics* **1989**, *37*, 73−78.
(41) Ivanov-Shits, A. K.; Kireev, V. V. *Kristallografiya* **2002**, *48*, 117−120.
(42) López, M. C.; Ortiz, G. F.; Lavela, P.; Tirado, J. L.; Stoyanova, R.; Zhecheva, E. *Chem. Mater.* **2013**, *25*, 4025−4035.